

Specific RNA binding to ordered phospholipid bilayers

Tadeusz Janas, Teresa Janas and Michael Yarus*

Department of Molecular, Cellular and Developmental Biology, University of Colorado, Boulder, CO 80309-0347, USA

Received February 20, 2006; Revised March 13, 2006; Accepted March 24, 2006

ABSTRACT

We have studied RNA binding to vesicles bounded by ordered and disordered phospholipid membranes. A positive correlation exists between bilayer order and RNA affinity. In particular, structure-dependent RNA binding appears for rafted (liquid-ordered) domains in sphingomyelin-cholesterol-1,2-dioleoyl-*sn*-glycero-3-phosphocholine vesicles. Binding to more highly ordered gel phase membranes is stronger, but much less RNA structure-dependent. All modes of RNA-membrane association seem to be electrostatic and headgroup directed. Fluorometry on 1,2-dimyristoyl-*sn*-glycero-3-phosphocholine liposomes indicates that bound RNA broadens the gel-fluid melting transition, and reduces lipid headgroup order, as detected via fluorometric measurement of intramembrane electric fields. RNA preference for rafted lipid was visualized and confirmed using multiple fluorophores that allow fluorescence and fluorescence resonance energy transfer microscopy on RNA molecules closely associated with ordered lipid patches within giant vesicles. Accordingly, both RNA structure and membrane order could modulate biological RNA–membrane interactions.

INTRODUCTION

It would be of great interest if there were an unexplored connection between RNA information and cellular membranes. For example, membrane affinity might localize the gene products of particular messages. Perhaps surprisingly, RNA sequences that bind the fluid (liquid disordered) phase of a phospholipid bilayer have previously been easily selected and characterized (1–3). In this case, consortia of several RNAs bind the bilayer as complexes. On this basis, a multi-subunit RNA membrane transporter specific for L-tryptophan has been constructed. Transporter properties suggest free RNA movement and thus dependence on a fluid membrane environment (4). Below, we characterize the affinity of RNA to vesicle

membranes containing phospholipid in more ordered states, using Fluorescence resonance energy transfer (FRET) microscopy, fluorescence spectroscopy and gel chromatography techniques.

Membrane phospholipids exist in four major states of order at temperatures close to physiological. The lamellar gel state (called L_{β}) is maximally ordered or frozen. Ripple gel (ordered, corrugated) phase (P_{β}), liquid-ordered (L_o) state and fluid (liquid disordered, liquid crystalline) state (L_{α}) progressively decline in order (5). A phospholipid membrane will pass from gel to ripple to fluid if temperature increases at equilibrium (6).

The intermediate liquid-ordered state above will be of particular importance below; there phospholipids diffuse freely within the bilayer (as in the fluid state), while keeping fatty acyl chains in an extended, kink-free conformation (as in ripple or gel states). Cholesterol can convert both gel and fluid phospholipid to liquid-ordered (7). In fact, a proposed role for cholesterol in animal plasma membranes is to reduce the tendency of membrane lipids to separate into fluid and gel phases by forming an intermediate liquid-ordered phase (8). At physiological temperatures, cellular membranes probably coexist as domains of fluid and liquid-ordered. This biological balance of states may itself be regulated (9,10). Liquid-ordered lipid clusters containing cholesterol and sphingolipids, surrounded by fluid glycerophospholipids are often called ‘rafts’ (11); such clusters are detectable, using several independent biochemical and biophysical assays, in animal plasma membranes [for review see (12)].

Sphingomyelin and cholesterol-rich regions in biological membranes can be readily documented via sphingolipid- or cholesterol-specific fluorescent probes (13). Probes specific for sphingolipids include cholera toxin B [specific for monosialoganglioside GM1 (14)] and the earthworm peptide lysenin [specific for sphingomyelin (15)].

Rafts may also be detected via their elevated cholesterol; probes specific for cholesterol include the polyene antibiotic filipin [from *Streptomyces filipinensis* (16)], the peptide perfringolysin [θ toxin (17)], the naturally occurring fluorescent cholesterol analog dehydroergosterol [DHE (18)] and fluorescent-labeled poly(ethylene glycol)-cholesteryl ethers [PEG-Chols (19)]. In the simpler synthetic membranes of

*To whom correspondence should be addressed. Tel: +1 303 492 8376; Fax: +1 303 492 7744; Email: yarus@colorado.edu

The authors wish it to be known that, in their opinion, the first two authors should be regarded as joint First Authors

© The Author 2006. Published by Oxford University Press. All rights reserved.

The online version of this article has been published under an open access model. Users are entitled to use, reproduce, disseminate, or display the open access version of this article for non-commercial purposes provided that: the original authorship is properly and fully attributed; the Journal and Oxford University Press are attributed as the original place of publication with the correct citation details given; if an article is subsequently reproduced or disseminated not in its entirety but only in part or as a derivative work this must be clearly indicated. For commercial re-use, please contact journals.permissions@oxfordjournals.org

giant lipid vesicles cholesterol/sphingomyelin rafts have been detected using peptide/antibiotic-fluorophores, fluorescent phospholipids, indocarbocyanine dyes and the planar dye perylene (20–23). Below we use these methods for visualization of ordered phospholipid to detect the relative dispositions of liquid-ordered (rafted) lipid patches and membrane-bound, selected RNAs.

MATERIALS AND METHODS

Materials

The following were purchased from Avanti Polar Lipids (Alabaster, AL): 1,2-dipalmitoyl-*sn*-glycero-3-phosphocholine (DPPC); 1,2-dimyristoyl-*sn*-glycero-3-phosphocholine (DMPC); 1,2-dimyristoleoyl-*sn*-glycero-3-phosphocholine (DMOPC); 1,2-dioleoyl-*sn*-glycero-3-phosphocholine (DOPC); cholesterol (CHOL); *N*-stearoyl-D-erythro-sphingosylphosphorylcholine (Stearoyl Sphingomyelin, SM), ovine brain ganglioside GM1. Fluorescent probes: DPH-HPC, RH-421, Pacific Blue-PE, YOYO-1, AlexaFluor555-CTB, Lissamine Rhodamine-PE were purchased from Molecular Probes (Eugene, OR). Perylene was from Sigma (St Louis, MO). RNA 10 (113mer; 2) serves in these experiments as a representative structure with no affinity for fluid membranes. RNA 80N (121mer, 80mer central randomized tract) similarly serves as a sample for simultaneous characterization of many RNA structures. RNA sequences were transcribed *in vitro* with T7 RNA polymerase, as described elsewhere (2).

Preparation of large unilamellar vesicles (LUV)

The appropriate lipids were dissolved in chloroform or chloroform/methanol (2/1) and solvent was evaporated under a stream of nitrogen gas, then desiccated under vacuum for at least 2 h. The lipids were resuspended in HEPES buffer (50 mM HEPES, 50 mM NaCl, 5 mM MgCl₂ and 2 mM CaCl₂, pH 7.0) or in HEPES buffer with varied NaCl concentration, and multilamellar liposomes were formed by gentle vortex. The suspension was subjected to seven freeze-thaw cycles by repeated immersion in liquid nitrogen followed by warming in 60°C water. LUV were prepared by extrusion using the Avanti MiniExtruder with a filter pore diameter of 100 nm.

Preparation of giant vesicles (GV)

GV used for fluorescence microscopy were prepared as described elsewhere (3). The lipids (DOPC, sphingomyelin, cholesterol, 250 nmol total) in chloroform/methanol and any fluorescent probe (0.2 mol% of lipids) were mixed, placed in a small glass vial, and dried using a weak stream of nitrogen to a thin film along the bottom of the vial. The vial was placed for 2 h in vacuum to remove residual solvents and HEPES buffer was added. The lipid thin layer was heated to 55°C (above the main phase transition of SM mixed with DOPC and cholesterol), hydrated under nitrogen and slowly cooled to room temperature for several hours. GV (2–10 μm) were collected from the upper layer of the solution.

Gel filtration: RNA–liposome binding assay

³²P-labeled RNA in water was denatured for 3 min at 65°C. HEPES buffer (50 mM NaCl, 50 mM HEPES, 5 mM MgCl₂

and 2 mM CaCl₂, pH 7.0) was added and RNA was folded by slow cooling to appropriate temperatures (18, 23 or 36°C). LUV were exposed to folded radiolabeled RNA (0.25 μM) for 5 min at appropriate temperature. Gel filtration of RNA/liposome mixture was performed using Sephacryl S-1000 Superfine (1.0 ml bed in a 1 ml plastic tuberculin syringe barrel), which admits lipid vesicles with diameters up to 300 nm for fractionation. The eluted fractions were analyzed for ³²P RNA content by scintillation counting and for liposomes by A₃₂₀ turbidity (2). Co-elution of RNA and liposomes indicates binding. Recovery of both vesicles and RNA was typically complete (>95%).

Anisotropy using fluorescence spectroscopy

Steady-state fluorescence anisotropy experiments on DPH (1,6 diphenyl-1,3,5-hexatriene)-HPC in 100 nm DMPC liposomes (1:100 mol ratio, probe: lipid) were performed on a Photon Technology International QM-2000-6SE fluorescence spectrometer using manual polarizers. Excitation and emission wavelengths were 384 and 429 nm, respectively. LUV (75 μM) in HEPES buffer were added to folded RNA and incubated for 15 min at mole ratio 75:1 (lipid:RNA). Fluorescence intensity was measured with the analyzing polarizer oriented parallel (I_{||}) or perpendicular (I_⊥) to the excitation polarizer, and anisotropy, *r*, was calculated:

$$r = \frac{I_{||} - gI_{\perp}}{I_{||} + 2gI_{\perp}},$$

where *g* represents an optical correction factor for slightly unequal horizontal and vertical polarized excitation intensities. Lipid vesicles in the absence of DPH-HPC were used to correct for light scattering.

Membrane dipole potential using fluorescence spectroscopy

Steady-state fluorescence experiments on an electric-field-sensitive dye RH-421 [*N*-(4-sulfobutyl)-4-(4-(4-(dipentylamino)phenyl)butadienyl)pyridinium, inner salt (24,25)] in 100 nm DMPC liposomes (1:200 mol ratio, probe/lipid) were performed on a Photon Technology International QM-2000-6SE fluorescence spectrometer. Lipid vesicles (75 μM) in HEPES buffer were added to folded RNA and incubated for 15 min at mole ratio 75:1 (lipid:RNA). For detecting changes in membrane electric field, a dual-wavelength ratiometric method was used (24), which takes advantage of the field's effect on differently oriented transition dipoles. Fluorescence was detected at 670 nm, at excitation 440 or 540 nm, and the ratio of fluorescence intensities, 440/540, was calculated.

FRET microscopy

RNA 10 at a final concentration of 87 nM in the HEPES buffer was mixed with the fluorescence dye YOYO-1 iodide (final concentration 910 nM). YOYO-1 is quite specific for nucleic acid, showing no observable fluorescence in the presence of vesicles alone. GV labeled with fluorescent probes were gently mixed with YOYO-labeled RNA at a volume ratio of 10:1, and mounted on glass coverslips. The images were collected on a Zeiss Axioplan2 fluorescence microscope (Carl Zeiss, Jena) with a 100× Plan-APO objective lens (numerical aperture 1.4).

Images were recorded with a Cooke SensiCam charge-coupled device camera and processed with the use of SlideBook software (Intelligent Imaging Innovations). The signals measured in the FRET channel (sensitized FRET) were corrected for crosstalk (26). In our system, ~24% of perylene emission, 17% of Pacific Blue-PE emission, 0.2% of YOYO excitation, 31% of YOYO emission, and 12% of the AlexaFluor555-CTB excitation, and 5% of the Lissamine Rhodamine-PE excitation were detected in the corresponding FRET channels.

RESULTS

RNA binding to highly ordered gel state membranes

We prepared liposomes from synthetic phosphatidylcholines having the same head-groups but different acyl chains and therefore different transition temperatures: DMPC (two 14-carbon saturated chains), DMOPC (two 14-carbon mono-unsaturated chains), DPPC (two 16-carbon saturated chains), and DOPC (two 18-carbon mono-unsaturated chains). Using these vesicles, we tested the affinity of ~120 nt RNAs to ordered lipid bilayers. We employed gel filtration that separates voided liposomes from included RNA. Two RNAs serve as models. RNA 10, a previously characterized structure which was shown not to bind detectably to a fluid phospholipid membrane (2,3), and RNA 80N, a 121mer with a central 80mer random sequence, which allows characterization of the behavior of many RNA sequences and structures simultaneously. 80N RNA was used as the initial pool for membrane RNA selection and also showed no significant binding to fluid phase phospholipid membranes (2).

Figure 1A shows a basic assay; free RNA 10 is retarded by Sephacryl S-1000 at 18°C. When incubated with DMPC liposomes (in ripple gel phase at this temperature), radiolabeled RNA 10 tracks the liposome peak (~80% binding). Thus, RNA 10 binds strongly to this highly ordered membrane. At the membrane transition temperature of 23°C (even mixture of ripple-gel and fluid phases; Figure 1B), the affinity of RNA 10 for DMPC liposomes is reduced (~58% binding) in comparison with 18°C, but still quite strong. In contrast, the melted, fully fluid DMPC membrane at 36°C (Figure 1C) binds little RNA (<0.1% co-migration).

Such temperature-dependent membrane binding does not reflect a temperature-dependent change in RNA structure. RNA 10 shows no association with other fluid phospholipid (phosphatidylcholine) bilayers: neither with DMOPC ($T_m = -2^\circ\text{C}$) liposomes at 18°C (Figure 2A) or 23°C (Figure 2B), nor with DOPC liposomes (also in fluid state, $T_m = -18^\circ\text{C}$) at 23 and 36°C (Figure 2B and C). However, the RNA affinity for DPPC liposomes (probably in the gel ripple phase at 36°C) is similar to DMPC liposomes tested at 18°C (in the same phase), despite the elevated temperature (Figure 2C). Therefore, RNA-membrane affinity varies with the gel-fluid state of the phospholipid, not the temperature.

Binding of RNA 10 and RNA 80N (Figure 3A) to DMPC liposomes at 18°C is reversible. RNA 10 bound to DMPC liposomes at 18°C, then incubated at 36°C for 10 min, shows only residual binding of ~2% on subsequent chromatography at 36°C (RNA 10 data not shown). Thus, RNA binding tracks the temperature-induced membrane transition precisely, decreasing as lipid order decreases.

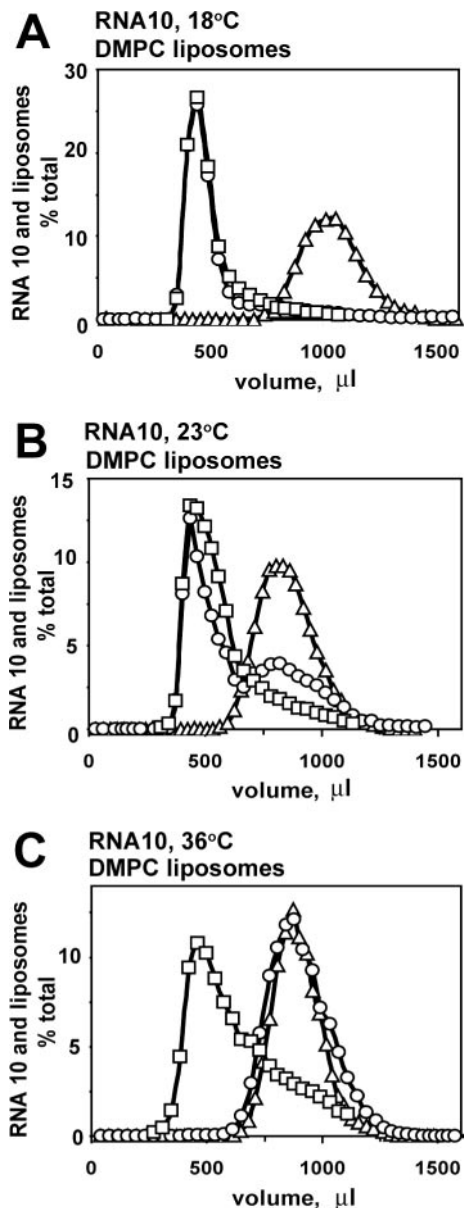


Figure 1. Temperature-dependence of RNA 10 binding to DMPC liposomes measured by gel filtration. Elution profiles at 18°C (A), 23°C (B), 36°C (C); triangles—RNA without liposomes; circles—RNA reacted with liposomes; squares—liposomes with RNA. RNA concentration 0.25 μM , liposome concentration 10 mg/ml.

The affinity of RNA 80N both for DMPC (18°C) and DPPC (36°C) bilayers in ripple gel phase declines with increased NaCl (Figure 3B). A similar effect is observed for DMPC bilayers at 23°C (Figure 3A), suggesting electrostatic interaction of RNA and ordered lipid phases. This is consistent with a salient role for the phosphocholine headgroup in RNA affinity for fluid membranes (1). Despite this salt sensitivity, a small, but measurable fraction of RNA sequences are bound at 150 mM salt, that is, at physiological ionic strength (1–3% of RNA; Figure 3B).

To characterize RNA effects on ordered phospholipids, we measured fluorescent anisotropy on DMPC liposomes labeled with DPH-HPC fluorescent lipid (Figure 4A). The fluorescent probe DPH is attached to the fatty acid hydrocarbon and buried

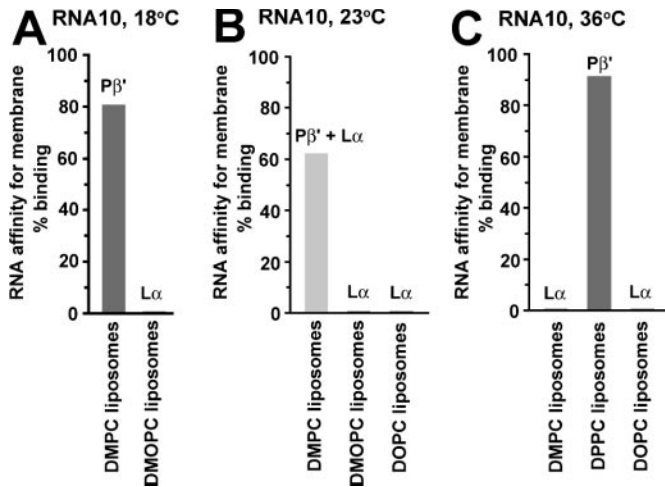


Figure 2. Effect of lipid bilayer order on RNA 10 affinity for large unilamellar phosphatidylcholine liposomes at 18°C (A), 23°C (B), 36°C (C); P β , lipid bilayer in ripple-gel phase; L α , lipid bilayer in liquid-disordered phase; P β + L α , lipid bilayer at the main phase transition temperature. RNA concentration 0.25 μ M, liposome concentration 10 mg/ml.

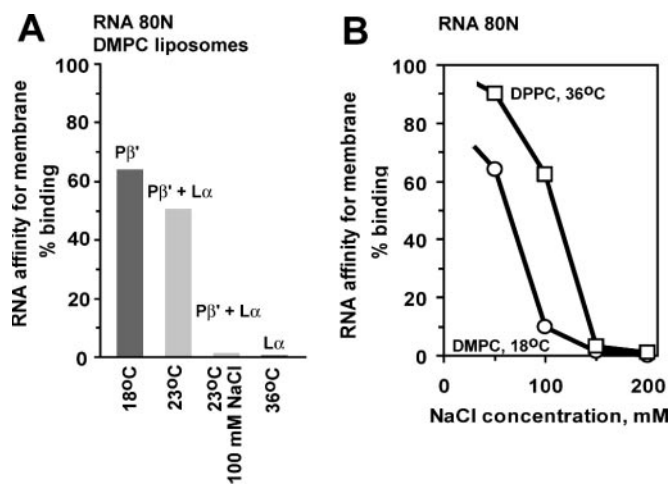


Figure 3. Effect of (A) temperature and (B) the ionic strength on RNA 80N binding to large unilamellar phosphatidylcholine liposomes. P β , lipid bilayer in ripple-gel phase; L α , lipid bilayer in liquid-disordered phase; P β + L α , lipid bilayer at the main phase transition temperature. RNA concentration 0.25 μ M, liposome concentration 10 mg/ml.

in the hydrophobic interior of the bilayer. Incubation of RNA 10 with DMPC liposomes (at molar ratio 1:75, RNA/phospholipid) broadens (by ~60%) the ripple gel-fluid phase transition, without shifting the transition temperature. Apparently, bound RNA interferes with, and lessens overall lipid cooperativity during the gel-fluid conversion.

Changes in membrane electric field were also followed by incorporating the oriented potential-sensitive RH-421 dye (24) (Figure 4B) and using the dual-wavelength ratiometric fluorescence method. Membrane-bound RNA 10 reduces (~10%) the membrane field below and at the ripple gel-fluid phase transition. This likely means (consistent with anisotropy above) that RNA interferes with head-group ordering, and thereby also supports a binding interaction between RNA and bilayer head-group dipoles.

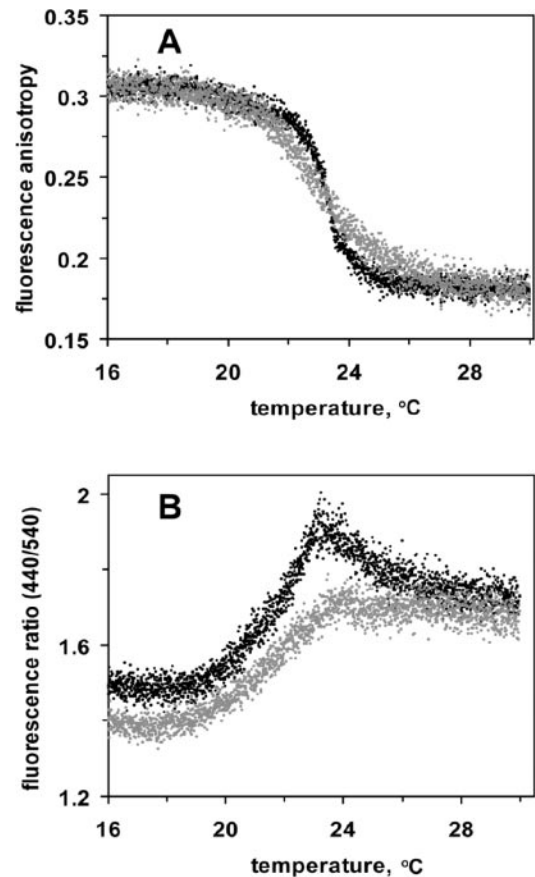


Figure 4. (A) Fluorescence anisotropy of DPH-HPC in DMPC liposomes in the presence (gray) and in the absence (black) of RNA 10; (B) Dipole-field-dependent ratio of fluorescence intensities, 440/540, of RH-421 in DMPC liposomes in the presence (gray) and in the absence (black) of RNA 10. Data were collected by temperature scanning at 1°C/min. RNA concentration 1 μ M, liposome concentration 75 μ M.

RNA binding to phospholipid rafts

Liposomes composed of ternary mixtures of lipids (unsaturated lipid, saturated lipid, cholesterol) exhibit phase separation (27) and can be used as models for multiple phases (microdomains, rafts) occurring in membranes of living cells (28). We studied the binding of RNA 10 and RNA 80N to raft-containing lipid vesicles composed of dioleoylphosphatidylcholine (DOPC), sphingomyelin (SM) and cholesterol (CHOL).

Figure 5A shows moderate (~17%) binding of RNA 10 to liposomes containing 60 mol% DOPC, 30 mol% of SM, and 10 mol% of CHOL using gel filtration at 23°C. Changing temperature to 36°C gave similar results (~15% binding). As shown in Figure 5B, cholesterol modulates the extent of RNA 10 binding (at constant 30 mol% SM) giving rise to the optimal (maximal) binding at 10 mol% CHOL in the ternary mixture. Therefore this membrane composition was chosen for fluorescence and FRET microscopy experiments below.

At higher than 10 mol% concentration, CHOL gradually reduces binding of RNA 10; with 30 mol% of CHOL, <3% of RNA is bound. This reduction probably results from contraction in liquid-ordered (raft) domains at higher membrane cholesterol concentrations (29,30). We observed a

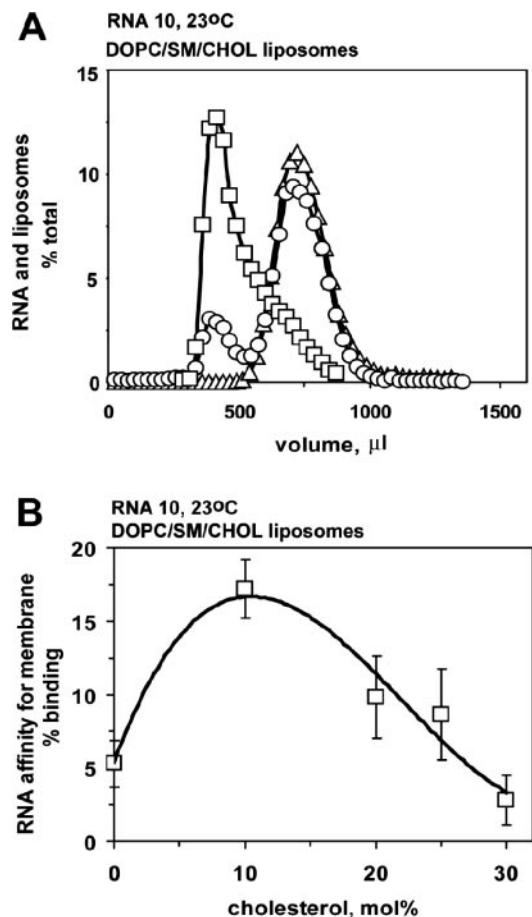


Figure 5. Cholesterol modulation of RNA 10 binding to LUV composed of DOPC/SM/CHOL. (A) Elution profiles obtained by gel filtration for DOPC/SM/CHOL (60:30:10 mol%, respectively) liposomes; triangles, RNA without liposomes; circles, RNA reacted with liposomes; squares, liposomes. (B) Cholesterol-dependence of RNA 10 binding to DOPC/SM/CHOL liposomes at constant (30 mol%) SM concentration. RNA concentration 0.75 μ M, liposome concentration 2.5 mg/ml.

qualitatively similar optimum for RNA 10 binding to LUV made of ternary mixtures of lipids held constant at 45% sphingomyelin. X-ray diffraction detects a single fluid phase at (1:1:1) DOPC/SM/CHOL (31) confirming that at higher cholesterol concentrations liquid-ordered domains (rafts) gradually disappear. At 0 mol% CHOL (70 mol% DOPC, 30 mol% SM) sphingomyelin domains in the gel state exist within the liquid-crystalline DOPC matrix (31,32) and the observed ~6% RNA 10 binding can be attributed to affinity for the SM gel state. We confirmed this affinity using an RNA-sphingomyelin liposome binding assay performed at 23°C (data not shown). These findings, taken together, suggest that RNA localization to raft (liquid-ordered) membrane domains could be controlled by changing the availability of rafted patches via local lipid composition.

We confirmed selective RNA 10 binding to lipid rafts using an independent technique—fluorescence and FRET microscopy applied to microscopically resolved giant (multi-micrometer) lipid vesicles. Below we show two kinds of experimental micrographs. In the first series (Figure 6A), bilayers were generally labeled using a blue dye—Pacific Blue attached to the head group of phosphatidylethanolamine

(PacBlue-PE), RNA 10 was labeled with green YOYO-1, which undergoes a large fluorescent enhancement upon intercalation into RNA structures (3), and lipid rafts were labeled with red AlexaFluor555 attached to cholera toxin B (AlexaFluor-CTB). A small amount (~0.1 mol%) of ganglioside GM1 was incorporated into the bilayer during vesicle formation. GM1 molecules strongly partition into rafts (14), so the red fluorescence of GM1-bound toxin can be used to visualize liquid ordered membranes (23).

Clearly, the green YOYO signal and the red raft signal are co-extensive in space, showing that the RNA has approximately uniformly coated the membrane's raft phase. In contrast, the RNA is present at much lower concentration, if at all, in the blue-only, or fluid membrane regions. This image, therefore, suggests selective RNA binding to rafts. Second, and at even finer resolution, we observe a strong FRET signal between YOYO and AlexaFluor (shown in false color in Figure 6A, VI). This image shows that the rafted lipid and the RNA are not just co-extensive, but in close (nanometer range) proximity, as they would be if RNA were floating in the rafted phospholipid membrane. This FRET signal is consistent with the separate locations of fluid and rafted membranes in merged images of YOYO and AlexaFluor (Figure 6A, IV). The presence of AlexaFluor-CTB itself does not change the affinity of RNA 10 for lipid vesicles (controls not shown; but see experiment just below). PacBlue PE does have some preference for liquid-disordered phase; however, this fractionation is rather weak (23). A detectable, but much more limited PacBlue→YOYO FRET (fluid→RNA) signal is visible (Figure 6A, V), which may result from contacts between sharply folded membranes.

In the second series of micrographs (Figure 6B), a new set of membrane reporters was used. Rafts were tagged with a blue dye—perylene (22), RNA 10 was labeled with YOYO-1, and fluid lipid bilayers incorporated a red dye (Lissamine Rhodamine) attached to the head group of phosphatidylethanolamine (LisRh-PE). Again, both coextension (suggesting mutual affinity) and a strong FRET signal coming from perylene (in rafts) to YOYO (in RNA) is visible (confirming intimate contact; Figure 6B, V). The FRET signal appears specific to ordered membrane in merged images of perylene and YOYO (Figure 6B, IV), and thereby shows that RNA-raft affinity is not dependent on cholera toxin (above). These experiments also seem to eliminate certain more complex RNA behaviors; e.g. that RNA might bind only to boundaries between raft and fluid domains. Again, a much smaller YOYO→LisRh FRET signal (by comparison to perylene→YOYO) is visible (Figure 6B, VI), probably again attributable to the juxtaposed fluid and rafted domains in some areas of these multilayered giant lipid vesicles.

To this point we have documented the affinity of RNA for rafted and gelled phospholipid domains. We now wish to show that these affinities, surprisingly, are distinct and in part, highly sensitive to RNA structure. Table 1 contains a survey of RNA structures, using RNAs related to the RNA 10 model, as well as RNAs of totally independent structure. While these data are not sufficient to closely define binding motifs, they show that there is an unanticipated difference in specificities. Binding of different RNAs to DMPC liposomes at 23°C (even mixture of gel and fluid) is (within experimental variation) ~50%, without regard to detailed RNA structure. This extends

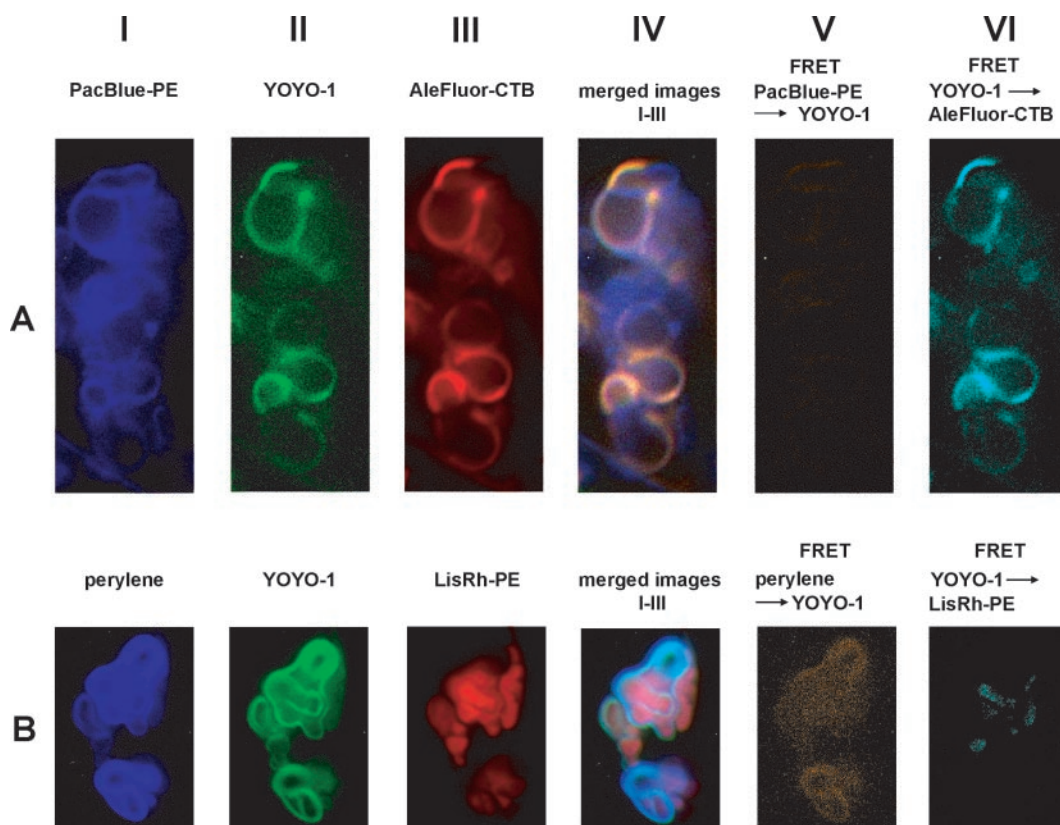


Figure 6. RNA 10 binding to liquid-ordered rafts visualized by FRET microscopy. (A) Blue, Pacific Blue-PE (PacBlue-PE) in giant lipid vesicles composed of DOPC/SM/CHOL (60:30:10 mol%, respectively) and 0.1 mol% of ganglioside GM1; green, YOYO-1 intercalated within RNA 10; red, AlexaFluor555 attached to cholera toxin B (AleFluor-CTB) bound to the ganglioside GM1 within liquid-ordered regions of giant lipid vesicles. (B) Blue, perylene in the liquid-ordered regions of giant lipid vesicles composed of DOPC/SM/CHOL (60:30:10 mol%, respectively); green, YOYO-1 intercalated in RNA 10; red, LissamineRhodamine-PE in giant lipid vesicle membranes. The width of the images is 8 μm .

even to the randomized sequences of RNA 80N, which comprise a varied sample of primary, and presumably higher order structures. Thus the ripple gel phase binds RNA almost without regard to superstructure, presumably via a multicharge—multidipole type of phospholipid—RNA interface, as discussed above.

In contrast, RNA binding to lipid rafts exhibits RNA-structure specificity. The computed RNA secondary structures in the table are the output of BayesFold, a Bayesian folding program (33). The highest level of binding (17 or 16%) was observed for RNA 10 and RNA 67-2, a derivative of RNA 10 having 8 nt changed within the left-hand hairpin loop. Apparently the leftward loop's sequence was not crucial to the RNA—raft association. However, changing the central part of RNA 10 by replacing 40 nt (in RNA 10_{Trp}, 4) or by 60 nt [in RNA 10_{Arg(D)5}] reduces raft binding to 9 and 2.2%. For the random pool of RNA sequences (RNA 80N) binding does not exceed 1%, similar to the unique structure, RNA Trp70-93 which has no sequence in common with RNA 10, being independently derived (34). Thus, RNA binding to CHOL-SM rafts varies at least 20-fold when RNA structure is varied. Definition of these ordered membrane-binding RNA substructures will likely require closely controlled sequence/structure comparisons.

Accordingly, RNA binding to gel phase phospholipid membranes appears to be nearly independent of detailed RNA primary, secondary and tertiary structure. Rafted

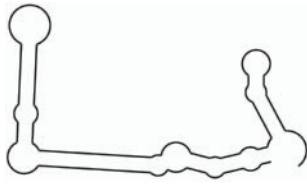
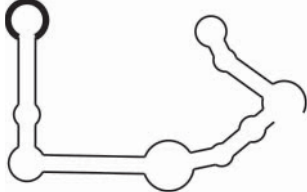

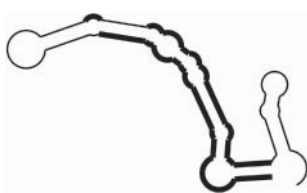

(liquid-ordered) membranes, in contrast, distinguish different RNA folds strongly, even when the estimated RNA structures do not appear distinctive to the experimental onlooker (Table 1).

DISCUSSION

Thus, we can correlate RNA affinity for membranes with phospholipid order. Taking randomized nucleotide sequences (with their 50% base pairing) as a rough-and-ready sample of 'all' RNA structures suggest that a greater fraction of RNA structures bind bilayers as phospholipid order increases: fluid < raft < ripple < gel. RNA binding to lipid ripple-gel phase (at the phase transition temperature) unexpectedly shows no significant RNA-structure specificity. On the other hand, a state of intermediate order (the liquid-ordered or rafted state, believed to occur in biological membranes) shows RNA-structure dependent affinity (Figures 5 and 6 and Table 1). Conceivably, this is attributable in part to the binding of RNA to a rigid phosphocholine lattice in the gel state, but to a conformable, more fluid receptor in rafts.

Reciprocally, RNA binding to ripple gels decreases both membrane electric field and fatty acyl chain-mediated cooperativity. Unpublished data suggest that the same is true of binding to rafted phospholipids. These data suggest that these RNAs prefer and stabilize different lipid arrangement(s)

Table 1. RNA binding to LUV composed of DMPC or DOPC/SM/CHOL (60:30:10 mol%, respectively)

Name of RNA	RNA length (nt)	RNA 2° structure calculated by BayesFold	RNA binding, % total DMPC LUV (gel + fluid phase)	RNA binding % total [DOPC/SM/CHOL] LUV (raft phase)
10	113		55	17
67-2	109		46	16
10 _{Trp}	114		50	9.0
10Arg(D)5	112		51	2.2
80N	121	varied	47	0.9
Trp 70-93	109		44	0.7

Binding assay was performed in HEPES buffer (50 mM HEPES, 50 mM NaCl, 5 mM MgCl₂ and 2mM CaCl₂, pH 7.0) at 23°C. The regions of RNA structures with changed nucleotides (in comparison with RNA 10) are in bold. For simplicity, the RNA unrelated to RNA 10 is shown completely bold, instead of broken by accidental matches. Line drawings are one output of BayesFold, a Bayesian RNA folding program (33).

than that in unbound ordered bilayers, thus paralleling our previous conclusions for fluid bilayers (3). RNA binding to all phospholipid bilayers is sensitive to ionic strength. These observations suggest an electrostatic affinity in the main, despite the observed difference in raft and gel specificity for RNA structures.

RNAs binding to ripple gel phase at physiological ionic strength (1–3%) implies that one must look through 30–100 molecules (or 2400–8000 nt) to find a binding structure. If we (very approximately) conceptualize the binding site as a linear sequence, this in turn suggests that structures that bind have approximately the prevalence expected of a particular

hexanucleotide ($4^{-6} = 1/4096$). Such a binding site implies that well-bound RNAs are rare among unselected RNAs, but makes it likely also that they will be easily selected at higher ionic strength, even as RNA structures that bound completely fluid phospholipid were rare, but easily selected (1–2). Initial rarity but easy selection also seems an ideal set of properties for evolution of controlled affinity between phospholipid membranes and biological RNAs.

Interestingly, given results of this work, there appears to be a parallel of surprising depth between RNA–membrane and peptide–membrane interactions. The protein phospholipase A₂ enzyme has particular affinity for the corrugations of the ripple

gel phase (35). Similarly, membrane RNAs (1–4) resemble some toxins and antimicrobial (bactericidal or fungicidal) water-soluble peptides [for a review see (36)] in preferential binding to lipid packing defects (37), more extensive binding to ripple gel than fluid phase (38), preferential binding to the edges of membrane pores (39), membrane destabilization (40), broadening of the transition temperature range and decreasing the slope of the transition (41), lowering of membrane internal electric field (42), and membrane pore formation (36). Most of these properties can now be duplicated by RNA–membrane examples.

Studies on the reconstituted membranes containing proteins have shown that proteins immobilize and order lipid hydrophobic chains adjacent to the protein molecule (12). On one hand, this parallels the effect of bound RNAs in changing the lipid state. On the other hand, we also speculate that re-ordered lipid associated with proteins may either attract or repel membrane RNAs. Therefore there may be, implicit in these results, a new directing principle for ordered nucleoprotein arrays on membrane surfaces.

One consequence of these parallels has to do with antibiotic activity. Because bacteria readily evolve resistance to antimicrobial peptides (43), this work suggests that nucleic acids might be useful additions to the antimicrobial armamentarium.

Scattered observations on nucleic acid affinity and membrane order preexist. Adsorption of radioactive poly(U) and tRNA to fluid mitochondrial and egg phosphatidylcholine liposomes has been detected (44) but at levels 100 times weaker than here, comparable with observed binding of RNA to fluid membranes. Conversely, stable binding of pTZ plasmid DNA (2880 bp) to a room temperature DPPC bilayer (gel phase), after overnight incubation at 4°C, has been reported (45) using atomic force microscopy. However, the authors were unable to detect binding of DNA to DMPC liposomes at 23°C (transition temperature, thus ripple gel plus fluid). Similar results appear (46) for binding of single-strand ~25 nt phosphorothioate oligonucleotides to phosphatidylcholine liposomes using a fluorescent dye specific for DNA: binding was higher for an ordered lipid bilayer.

Finally, in considering possible controlled membrane affinity for RNAs in living cells, this work raises the possibility that RNA-membrane association might be varied by selection of suitable RNA structures (or might be modulated via small RNA or small-molecule RNA ligands) as well as by varying the composition and order of phospholipids in different cellular membrane domains. Bound RNAs in turn will change the local bilayer structure and activities, whether in fluid or more ordered phospholipid patches.

ACKNOWLEDGEMENTS

We thank Dr J. Richard McIntosh (University of Colorado, MCD Biology) for the use of his fluorescence microscope, and also Dr Joseph J. Falke (University of Colorado, Department of Chemistry and Biochemistry) for use of his spectrofluorometer. This work was supported by NIH Research Grant GM-30881. Funding to pay the Open Access publication charges for this article was provided by NIH GM-30881

Conflict of interest statement. None declared.

REFERENCES

1. Khvorova, A., Kwak, Y.G., Tamkun, M., Majerfeld, I. and Yarus, M. (1999) RNAs that bind and change the permeability of phospholipid membranes. *Proc. Natl Acad. Sci. USA*, **96**, 10649–10654.
2. Vlassov, A., Khvorova, A. and Yarus, M. (2001) Binding and disruption of phospholipid bilayers by supramolecular RNA complexes. *Proc. Natl Acad. Sci. USA*, **98**, 7706–7711.
3. Janas, T. and Yarus, M. (2003) Visualization of membrane RNAs. *RNA*, **9**, 1353–1361.
4. Janas, T., Janas, T. and Yarus, M. (2004) A membrane transporter for tryptophan composed of RNA. *RNA*, **10**, 1541–1549.
5. Lewis, R.N.A.H. and McElhaney, R.N. (2005) The mesomorphic phase behavior of lipid bilayers. In Yeagle, P.L. (ed.), *The structure of biological membrane*. CRC Press, Boca Raton, pp. 53–120.
6. Koynova, R. and Caffrey, M. (1998) Phases and phase transitions of the phosphatidylcholines. *Biochim. Biophys. Acta*, **1376**, 91–145.
7. Simons, K. and Vaz, W.L.C. (2004) Model systems, lipid rafts, and cell membranes. *Annu. Rev. Biophys. Biomol. Struct.*, **33**, 269–295.
8. McMullen, T.P.W., Lewis, R.N.A.H. and McElhaney, R.N. (2004) Cholesterol–phospholipid interactions, the liquid-ordered phase and lipid rafts in model and biological membranes. *Curr. Opin. Colloid Interface Sci.*, **8**, 459–468.
9. Hazel, J.R., McKinley, S.J. and Gerrits, M.F. (1998) Thermal acclimation of phase behavior in plasma membrane lipids of rainbow trout hepatocytes. *Am. J. Physiol.*, **275**, R861–R869.
10. Deshni, P., Gombos, Z., Nishiyama, Y. and Murata, N. (1997) The action *in vivo* of glycine betaine in enhancement of tolerance of *Synechococcus* sp. strain PCC 7942 to low temperature. *J. Bacteriol.*, **179**, 339–344.
11. Simons, K. and Ikonen, E. (1997) Model systems, lipid rafts, and cell membranes. *Nature*, **387**, 569–572.
12. McConnell, H.M. and Vrljic, M. (2003) Liquid-liquid immiscibility in membranes. *Annu. Rev. Biophys. Biomol. Struct.*, **32**, 469–492.
13. Ishitsuka, R., Sato, S.B. and Kobayashi, T. (2005) Imaging lipid rafts. *J. Biochem.*, **137**, 249–254.
14. Stauffer, T.P. and Meyer, T. (1997) Compartmentalized IgE receptor-mediated signal transduction in living cells. *J. Cell Biol.*, **139**, 1447–1454.
15. Kiyokawa, E., Baba, T., Otsuka, N., Makino, A., Ohno, S. and Kobayashi, T. (2005) Spatial and functional heterogeneity of sphingolipid-rich membrane domains. *J. Biol. Chem.*, **280**, 24072–24084.
16. Sokol, J., Blanchette-Mackie, E.J., Kruth, H.S., Dwyer, N.K., Amende, L.M., Butler, J.D., Robinson, E., Patel, S., Brady, R.O., Comly, M.E., Vanier, M.T. *et al.* (1988) Type C Niemann-Pick disease—Lysosomal accumulation and defective intracellular mobilization of low density lipoprotein cholesterol. *J. Biol. Chem.*, **263**, 3411–3417.
17. Waheed, A.A., Shimada, Y., Heijnen, H.F., Nakamura, M., Inomata, M., Hayashi, M., Iwashita, S., Slot, J.W. and Ohno-Iwashita, Y. (2001) Selective binding of perfringolysin O derivative to cholesterol-rich membrane microdomains (rafts). *Proc. Natl Acad. Sci. USA*, **98**, 4926–4931.
18. Mukherjee, S., Zha, X., Tabas, I. and Maxfield, F.R. (1998) Cholesterol distribution in living cells: fluorescence imaging using dehydroergosterol as a fluorescent cholesterol analog. *Biophys. J.*, **75**, 1915–1925.
19. Sato, S.B., Ishii, K., Makino, A., Iwabuchi, K., Yamaji-Hasegawa, A., Senoh, Y., Nagaoka, I., Sakuraba, H. and Kobayashi, T. (2004) Distribution and transport of cholesterol rich membrane domains monitored by a membrane-impermeant fluorescent polyethylene glycol-derivatized cholesterol. *J. Biol. Chem.*, **279**, 23790–23796.
20. Dietrich, C., Bagatolli, L.A., Volovyk, Z.N., Thompson, N.L., Levi, M., Jacobson, K. and Gratton, E. (2001) Lipid rafts reconstituted in model membranes. *Biophys. J.*, **80**, 1417–1428.
21. Samsonov, A.V., Mihalyov, I. and Cohen, F.S. (2001) Characterization of cholesterol-sphingomyelin domains and their dynamics in bilayer membranes. *Biophys. J.*, **81**, 1486–1500.
22. Baumgart, T., Hess, S.T. and Webb, W.W. (2003) Imaging coexisting fluid domains in biomembrane models coupling curvature and line tension. *Nature*, **425**, 821–824.
23. Bacia, K., Schwille, P. and Kurzchalia, T. (2005) Sterol structure determines the separation of phases and the curvature of the

- liquid-ordered phase in model membranes. *Proc. Natl Acad. Sci. USA*, **102**, 3272–3277.
24. Clarke, R.J. and Kane, D.J. (1997) Optical detection of membrane dipole potential: avoidance of fluidity and dye-induced effects. *Biochim. Biophys. Acta*, **1323**, 223–239.
 25. Clarke, R.J. and Lupfert, C. (1999) Influence of anions and cations on the dipole potential of phosphatidylcholine vesicles: a basis for the Hofmeister effect. *Biophys. J.*, **76**, 2614–2624.
 26. Sorkin, A., McClure, M., Huang, F. and Carter, R. (2000) Interaction of EGF receptor and Grb2 in living cells visualized by fluorescence resonance energy transfer (FRET) microscopy. *Curr. Biol.*, **10**, 1395–1398.
 27. Mukherjee, S. and Maxfield, F.R. (2004) Membrane domains. *Annu. Rev. Cell Dev. Biol.*, **20**, 839–866.
 28. Edidin, M. (2003) The state of lipid rafts: from model membranes to cells. *Annu. Rev. Biomol. Struct.*, **32**, 257–283.
 29. Feigenson, G.W. and Buboltz, J.T. (2001) Ternary phase diagram of dipalmitoyl-PC/dilauroyl-PC/cholesterol: nanoscopic domain formation driven by cholesterol. *Biophys. J.*, **80**, 2775–2788.
 30. Lawrence, J.C., Saslow, D.E., Edwardson, J.M. and Henderson, R.M. (2003) Real-time analysis of the effects of cholesterol on lipid raft behavior using atomic force microscopy. *Biophys. J.*, **84**, 1827–1832.
 31. Gandhavani, M., Allende, D., Vidal, A., Simon, S.A. and McIntosh, S.A. (2002) Structure, composition, and peptide binding properties of detergent soluble bilayers and detergent resistant rafts. *Biophys. J.*, **82**, 1469–1482.
 32. Veatch, S.L. and Keller, S.L. (2005) Miscibility phase diagrams of giant vesicles containing sphingomyelin. *Phys. Rev. Lett.*, **94**, 148101.
 33. Knight, R., Birmingham, A. and Yarus, M. (2004) BayesFold: rational 2° folds that combine thermodynamic, covariation, and chemical data for aligned RNA sequences. *RNA*, **10**, 1323–1336.
 34. Majerfeld, I. and Yarus, M. (2005) A diminutive and specific RNA binding site for L-tryptophan. *Nucleic Acids Res.*, **33**, 5482–5493.
 35. Leidy, C., Mouritsen, O.G., Jørgensen, K. and Peters, G.H. (2004) Evolution of a rippled membrane during phospholipase A₂ hydrolysis studied by time-resolved AFM. *Biophys. J.*, **87**, 408–418.
 36. Brogden, K.A. (2005) Antimicrobial peptides: pore formers or metabolic inhibitors in bacteria? *Nature Rev. Microbiol.*, **3**, 238–250.
 37. Barlic, A., Gutierrez-Aguirre, I., Caaveiro, J.M.M., Cruz, A., Ruiz-Arguello, M.B., Perez-Gil, J. and Gonzalez-Manas, J.M. (2004) Lipid phase coexistence favors membrane insertion of equinatoxin-II, a pore-forming toxin from *Actinia equina*. *J. Biol. Chem.*, **279**, 34209–34216.
 38. Castanho, M.A.R.B., Prieto, M. and Jameson, D.M. (1999) The pentaene macrolide antibiotic filipin prefers more rigid DPPC bilayers: a fluorescence pressure dependence study. *Biochim. Biophys. Acta*, **1419**, 1–14.
 39. Huang, H.W., Chen, F.Y. and Lee, M.T. (2004) Molecular mechanism of peptide-induced pores in membranes. *Phys. Rev. Lett.*, **92**, 198304.
 40. Bonev, B.B., Lam, Y.H., Anderluh, G., Watts, A., Norton, R.S. and Separovic, F. (2003) Effects of the eukaryotic pore-forming cytotoxin equinatoxin II on lipid membranes and the role of sphingomyelin. *Biophys. J.*, **84**, 2382–2392.
 41. Mancheno, J.M., Onaderra, M., del Pozo, A.M., Diaz-Achirica, P., Andreu, D., Rivas, L. and Gavilanes, J.G. (1996) Release of vesicle contents by an antibacterial cecropin A-melittin hybrid peptide. *Biochemistry*, **35**, 9892–9899.
 42. Shapovalov, V.L., Kotova, E.A., Rokitskaya, T.I. and Antonenko, Y.N. (1999) Effect of gramicidin A on the dipole potential of phospholipid membranes. *Biophys. J.*, **77**, 299–305.
 43. Buckling, A. and Brockhurst, M. (2005) RAMP resistance. *Nature*, **438**, 170–171.
 44. Budker, V.G., Godovikov, A.A., Naumova, L.P. and Slepneva, I.A. (1978) Interaction of polynucleotides with natural and model membranes. *FEBS Lett.*, **95**, 143–146.
 45. Malghani, M.S. and Yang, J. (1998) Stable binding of DNA to zwitterionic bilayers in aqueous solutions. *J. Phys. Chem.*, **102**, 8930–8933.
 46. Lu, D. and Rhodes, D.G. (2002) Binding of phosphorothioate oligonucleotides to zwitterionic liposomes. *Biochim. Biophys. Acta*, **1563**, 45–52.